MASTER

UCRL- 84234
PREPRINT

STRUCTURAL SUPPORT OF A YIN-YANG MAGNET FOR A TANDEM MIRROR REACTOR WITH THERMAL BARRIERS

John L. Erickson
Irving U. Ojalvo
John O. Myall

This paper was prepared for inclusion in the Proceedings of the Fourth ANS Topical Meeting on The Technology of Controlled Nuclear Fusion, King of Prussia, PA, October 14-17, 1980.

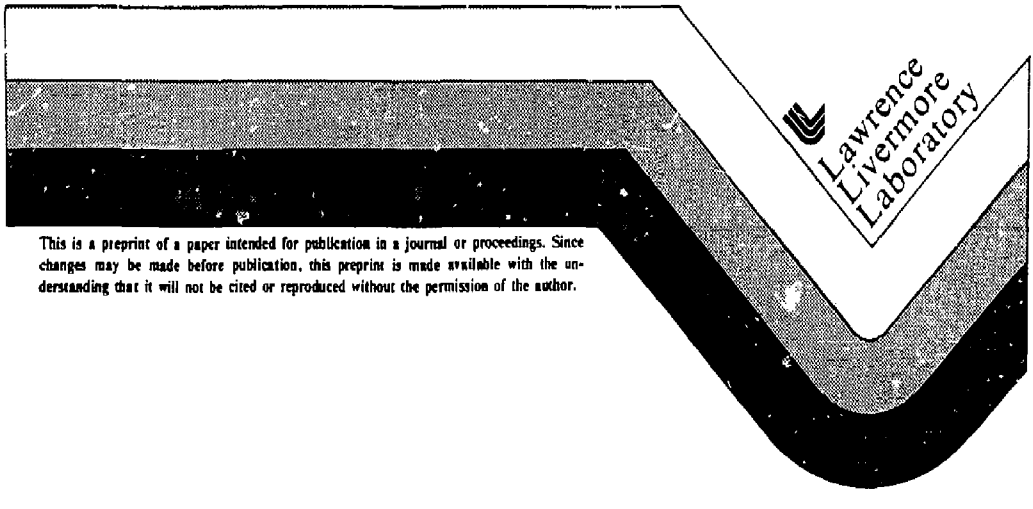

This is a preprint of a paper intended for publication in a journal or proceedings. Since changes may be made before publication, this preprint is made available with the understanding that it will not be cited or reproduced without the permission of the author.

DISTRIBUTION OF THIS DOCUMENT IS UNLIMITED

DISCLAIMER

STRUCTURAL SUPPORT OF A YIN-YANG MAGNET FOR A TANDEM MIRROR REACTOR WITH THERMAL BARRIERS*

By John L. Erickson, Irving U. Ojalvo** and John O. Myall***
Grumman Aerospace Corp., Bethpage, NY 11714

Conceptual designs of mirror power reactors have historically used high-field magnets that required massive restraining structures,[1,2] in addition to the basic coil case, to support the electromagnetic loads. Recently, application of the thermal barrier concept to tandem mirrors[3] has sufficiently improved reactor performance such that a yin-yang reactor magnet (Fig. 1) may not require significantly higher technology than is required for the Mirror Fusion Test Facility (MFTF) yin-yang coils.[4]

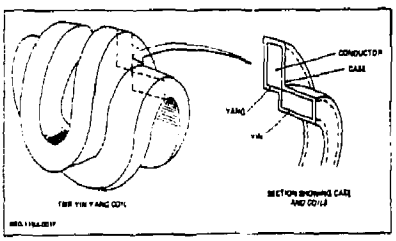

Fig. 1 Yin-yang magnet windings.

The approach taken in our study was to use a simple coil case of compact design and to add and modify structural members to transfer loads from one coil to the other. It has been assumed that the magnet assembly will resemble the MFTF design (Fig. 2). The structural material selected is 304 LN stainless steel with a yield stress of 120 ksi at 4° K. The niobium-titanium conductor is assumed to be of square cross-section to allow winding in two planes.

This report contains a comprehensive summary covering work performed by Grumman Aerospace Corporation, in conjunction with the Lawrence Livermore National Laboratory, on the TMF yin-yang coils. The yin-yang coil pair used for our analysis has a major arc radius of 2.7 m and a minor arc radius of 1.18 m, compared with

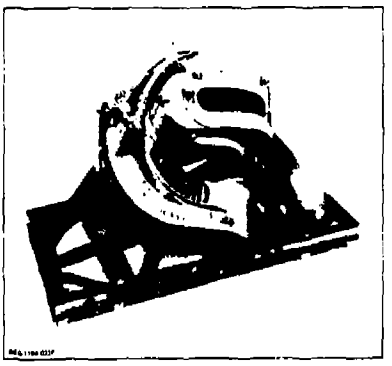

Fig. 2 MFTF yin-yang coil pair.

2.5 m and 0.75 m for the MFTF (see Table 1). The maximum field on the present conductor is 9.05 Tesla. This magnetic field is created by, and interacts with, a conductor current which produces a 360 million Newton total force, tending to separate the parallel lobes of the major arcs.

Structural Design Considerations

As will be described later, the region of highest stress in the coil case has generally been found located near the center of the minor arc. This peak stress is most often caused by in-plane bending, as the larger lobe separating forces are carried by moments in the minor arc. Thus, from a purely structural point of view, the optimal way to reduce this stress is by directly connecting the major radii of the same coil together with intracoil stiffening structure. However, because the plasma fan spreads rapidly as it leaves the major arc of the coil pair, this load path is not available for the placement of support structure. In addition, since the superconducting coil structure must be maintained at 4° K and the plasma heating of the first wall is very intense, a thermal/radiation shield of the order of 50 cm thickness is required between them, which further restricts this region for

* Work performed under the auspices of the U.S. Department of Energy by the Lawrence Livermore National Laboratory under contract number W-7405-ENG-48.
** Presently at Perkin-Elmer.
*** Lawrence Livermore National Laboratory

Parameter	MFTF	TMR
Major Arc Radius	2.5m	2.7m
Minor Arc Radius	0.75m	1.18m
Conductor Cross-Section	0.9m x 0.36m	2.1m x 0.36m*
Coil Section Current Density	2525 A/cm^2	2330-2500 A/cm^2**
Maximum Conductor Field	7.68 Tesla	9.04 Tesla
Lobe Spreading Force	100 x 10^6 Newtons	360 x 10^6 Newtons
Mirror Length	3.6m	4.9m
Vacuum Center Field	2T	4T
Mirror Ratio	2.1	1.5
Conductor Wt (both coils)	54,430 kg	201,000 kg

* increased to 2.1 x 0.44m at center of minor radius

** 2330 A/cm^2 for inner coil, 2500 A/cm^2 for outer coil

RSO-1194-024P

Table 1 Comparison of coil parameters: MFTF vs. TMR.

structural stiffening. For the TMR application, we have not considered any intracoil structure approach to be feasible. However, several NASTRAN finite element structural analysis runs, described later, were run to demonstrate the effectiveness of this latter method of support.

An initial set of NASTRAN runs was used to get a feel for the behavior of the structural support concepts by varying the use of inter- and in racoil structure. Assuming a uniform 4-in. case thickness as a basis, eight support variations were examined. In all cases, the maximum stresses occurred in the small radius.

We started with four intercoil connectors (gussets) for the entire coil pair, one at the center of each arc. This represented the minimum number of such supports considered for the entire coil pair. The stiffness of these gussets did not significantly affect the maximum stress level which was predominantly due to in-plane bending. We then located such gussets at 15°, 12°, and, finally, 3° intervals of arc. Distributing the intercoil supports around the coil made the coil pair behave quite differently. Although the maximum stress still occurred in the minor radius, and although the stress was reduced for each run having additional stiffeners, the factor contributing most to the stress changed from in-plane bending-produced to axial load-produced stress.

The last variation in the initial set of runs was to connect the major arc lobes of each coil together (an intracoil connector), in addition to the minimum intercoil connectors every 90°. These intracoil connectors, placed in the plasma stay-out zone, reduced the case stress to 10% below what had been attained with intercoil connectors every 3° of arc.

Since all of the computer runs in the first set of analyses had unacceptably high case stresses, the basic 4-in. case thickness was increased for the second set of runs (Fig. 3).

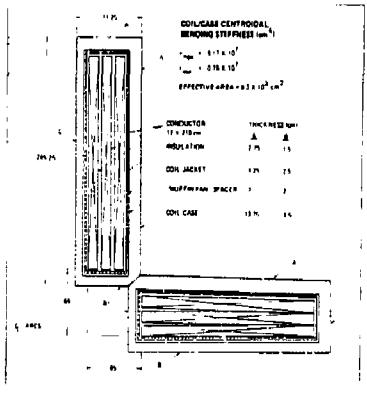

Fig. 3 Coil case properties detailed

In addition to strengthening the case, we added an axially-continuous angle bracket between the two coil cases to both transfer and help carry loads. This configuration also had gussets to

provide good coil-to-coil stiffness and is shown in Figure 4. By firmly fastening the angle bracket to each coil case to permit efficient load transfer, the case stresses were reduced to more acceptable levels. The conductor bending stiffness was ignored in all cases. The stretching stiffness was included in the uniformly thick cases, but not in the non-uniform cases.

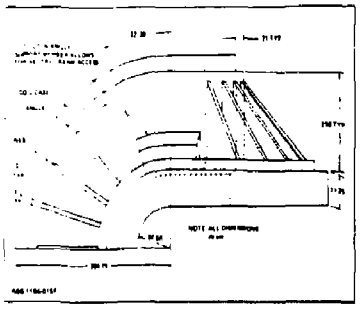

Fig. 4 Preliminary design with 15-degree spaced intercoil stiffeners

The third set of runs was used to study local reinforcement of the minor arc region to increase its bending strength. A structure such as that shown in Figure 5 accomplishes two things. First, it increases bending strength for in-plane loads in the minor arc. Second, its box-like extension takes loads directly from the major arc of the adjacent coil and transfers them to the reinforced coil where they are carried as in-plane bending in the major arc. The eccentric load path of an angle-shaped intercoil structure is avoided so that torsion in the case is reduced. Using the stiffness of the 8-1/4" thick angle of Figure 4 as a base, a series of runs examined the effect of making such minor radius reinforcement 10 times as stiff over various fractions of the arc. A factor of 3 times the angle stiffness is a practical limit using a box beam section with 8-1/4" uniformly thick walls.

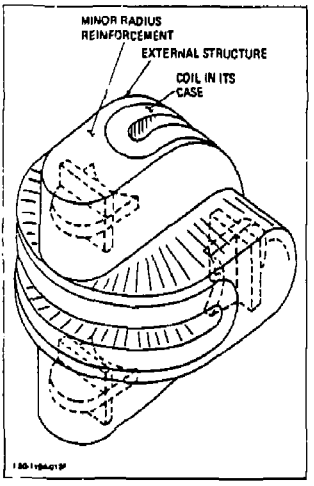

Fig. 5 Small radius reinforcement design.

Structural Model

Coil and Support Elements

Each coil is composed of two large and two small semi-circular, planar, connected arcs as was shown in Figure 1. The smaller arcs are parallel to one another and are perpendicular to the larger arcs. Projections of the TMR yin-yang end-plug magnet centerlines are shown in Figure 6. Because of the geometrical and loading symmetry, it was not necessary to model the entire coil. For analysis purposes, the one-quarter symmetric model shown in Figure 6 was selected. A total of 30 smaller equal-lengthed straight beam elements and 30 longer equal lengthed beam elements were used to construct two planar circular arcs for each coil. Figure 6 indicates the node-numbering sequence for the two one-quarter coil models.

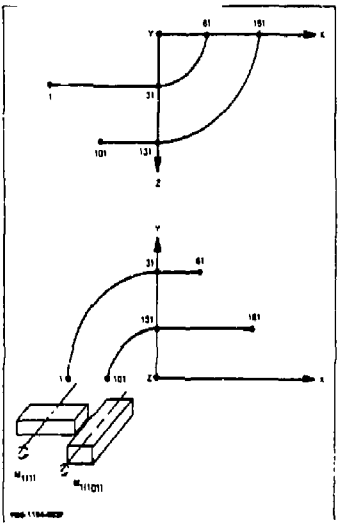

Fig. 6 One-quarter stick models of each TMR coil.

Besides modeling the coils and their cases, the system support structure required special treatment. Three distinct types of structural support systems were considered, as well as various combinations of these. The first type of support system which was investigated is "intercoil" stiffening and refers to connections between the two coils. The second type of support system involves the use of stiffeners to

connect one part of a coil to another part of the same coil. The third generic type of stiffener is associated with a curved beam that is similar in shape to the yin and yang coils and is contained midway between them (Fig. 7). Its purpose is to act as a curved beam support for each coil. This type of coil requires some type of connection to the coils as well, but this attachment is not shown in Figure 7. As mentioned earlier, each of these type stiffeners,

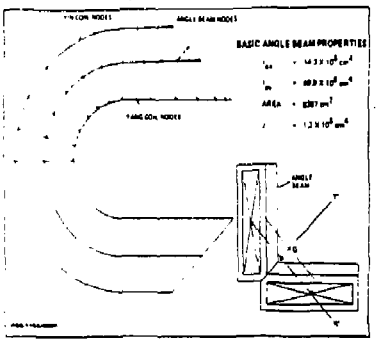

Fig. 7 Finite element model of coils with angle connecting beam.

as well as various combinations of them, were considered in the trade studies to be described.

Since the main point of this study was to establish design feasibility and efficacy of the different support systems, simple beam elements were again used to represent the stiffeners.

Electromagnetic Loads

The electromagnetic loads data on the yin-yang coil centerline were developed at the Lawrence Livermore National Laboratory. The numerical results were obtained using the EFFI code (Ref. 5). The applied loads are plotted in Figure 8 as inplane and out-of-plane running

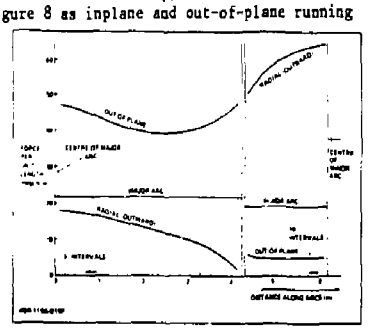

Fig. 8 EM loads on coil arcs

load components on the semi-major and semi-minor arcs. The center of each arc is denoted on either end of Figure 8. The inplane load components are directed radially outward and are largest on the smaller arcs. The out-of-plane loads on each coil act to open each coil at both the smaller and larger arcs, but the effect is more pronounced at the smaller arcs since the load components are much larger along the larger semi-circles. The running load component projections are drawn, approximately to scale, on the coil arcs in Figure 9.

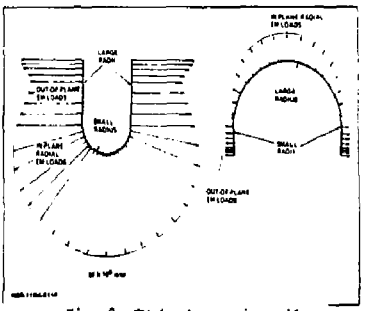

Fig. 9 EM loads on yin coil.

In preparing input for the structural model, it was necessary to multiply the local running load components by the length of coil arc associated with each node, to decompose the inplane loads into Cartesian coordinates and to apply them at the structural model nodes. Application of the load in this manner, directly to the coil cases, assumes that the conductors fit snugly within their structural cases and so pass their local body loadings directly to them. However, an important exception to this was considered whereby the small arcs' inplane radial loads were assumed to be carried entirely by the conductors themselves, rather than their cases. This situation could be physically realized if there were sufficient clearance between the outside of the conductor bundle and the inner wall of the case of the small radius arcs, so that the case would not contact the coil as the small arc of the conductor bundle developed hoop stress and expanded radially. These outward forces could be reacted eventually by inplane radial loads on the large case arcs. It was assumed that the large arc reaction loads were uniformly distributed resulting in the net case loads depicted in Figure 10.

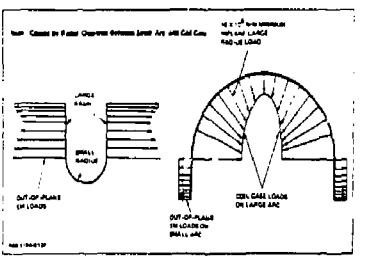

Fig. 10 EM loads on yin coil case.

Analysis Results

Numerical Results

A series of numerical studies were performed on the IBM 370/168 computer using the cosmic verion of the NASTRAN structural analysis computer code (Ref. 6), and the models described earlier. From a perusal of computer run output, it was rapidly determined that the critically stressed coil section was located at the center of the smaller arcs, and that the peak stresses were caused by a combination of direct and bending loads.

The initial structural model data submittals involved a series of trial cases in which the coil supports involved either discrete intercoil stiffening only or intracoil stiffening. The stiffnesses of the connecting members were varied, being made both large and small compared to the case properties, to ascertain the effect of stiffness upon case stresses.

The first set of results generated for the 4-in. uniform wall thickness case revealed that the preferred design approach for supporting the electromagnetic loads was through the use of intracoil stiffening (see cases 3 and 4 of Table 2). As may be seen, this type of support tends to reduce peak stress levels by a factor of 3. Unfortunately, the use of direct intracoil stiffeners interferes with the shape of the plasma which fans out between the large circular arcs. Therefore, further studies using intracoil stiffening were not considered.

The other observation that is evident from the results of Table 2 is that intercoil supports become more effective as they are made stiffer. As only two intercoil stiffeners were used for cases 1 and 2 of Table 2, additional stiffeners were employed. The results of using intercoil stiffeners every 15, 9, 6 and 3 degrees of arc are presented in Table 3. As may be seen, these results indicate an improvement in peak stress with increased intercoil stiffness.

Also included in Table 3 are the results from employing a continuous angle connector (Fig. 4). Once again, this type of stiffening is seen to reduce coil case stresses significantly and the improvement is strongly dependent upon the stiffness of the support angle employed. Table 4 shows the intercoil and angle stiffening connection effects upon the nonuniform case design (Fig. 3).

Up to this point, only the results for the loading of Figure 9 have been presented. Table 5 indicates the effect of employing coil case clearance at the outer radius of the small arc, resulting in the coil case loading of Figure 10. These results, when compared with those for the load case of Figure 9 (no coil/case clearance), indicate that the clearance design feature is an effective manner for reducing peak case stresses. The results, for a factor of 3 stiffening angle property-multiplier, were generated because it was felt that this was a

Case No.	Description	Stress (ksi) at Center of Large Radius				Stress (ksi) at Center of Small Radius			
		P/A	Bending	Components	Peak	P/A	Bending	Components	Peak
1	Four flexible connections at arc centers between coils	20	66	28	115	47	537	31	615
2	Two stiff connections at arc centers between coils	24	115	75	213	24	447	54	524
3	Same as Case 1 + 2 stiff intra-coil supports at the center of the major arcs assisting the small radii	40	66	51	137	31	88	45	163
4	Same as Case 2 + 2 stiff intra-coil supports at the center of the major arcs assisting the small radii	19	51	44	114	31	87	44	162

RSG-1184-013P

Table 2 TMR yin-yang coil case stresses for a uniform 4 inch wall thickness case.

Case No.	Description		Stress (ksi) At Center of Large Radius				Stress (ksi) At Center of Small Radius			
			P/A	Bending	Components	Peak	P/A	Bending	Components	Peak
1	Soft Inter:	Four soft connections at arc centers between coils	20	66	28	115	47	537	31	615
2	Stiff Inter:	Four stiff connections at arc centers between coils	24	115	75	213	24	447	5.	52.
5	Stiff 2:	Stiff connections every 15° of arc between coils	9	92	11	102	77	9?	3?	[illegible]
6	Stiff 3:	Stiff connections every 6° to 9° of arc between coils	15	60	5	80	83	72	-?	200
7	Soft 2:	Soft connections every 15° of arc between coils (100 times softer than for "stiff 2"	32	211	11	25.	36	29?	-	3??
8	Stiff 5:	Stiff connections every 3° of arc between coils	20	43	3	8.	89	.9	--	181
9	Angle 1:	Continuous angle connection between coils	25	91	1	118	38	1.0	1.	212
10	Angle 2:	Same as "Angle 1" except that angle stiffness properties are double	22	56	1	79	38	9?	29	1.8
11	Angle .5:	Same as "Angle 1" except that angle stiffness properties are a factor of 10 higher	12	9	4	24	35	2?	.9	79

ORNL-DWG-1184-01AP

Table 3 TMR yin yang coil case stresses for a 4-inch stresses for a 4-inch wall and no intracoil stiffening

more realistic design possibility, whereas a factor of 10 property-multiplier was less realistic. It is interesting to note that the use of a stiff angle over only 40 percent of the coil, with the loads of Figure 10, is almost as effective as if this angle existed over the entire coil (see cases 16.1 and 16.2 of Table 5).

Discussion of Numerical Results

In comparing the preliminary structural requirements of the TMR yin-yang coils with results of the present conceptual design and analysis study, it appears that the proposed concept listed as case 16.1 of Table 5 is only marginally acceptable. It has been customary, in similar studies, to select a peak nominal stress of two-thirds the yield stress as a design criterion. Note, however, that a number of considerations must be investigated before accepting or rejecting the present concept on purely structural grounds. For example, the ultimate stress for the contemplated case material is between 250 and 300 ksi, which is more than twice the yield stress. This fact might permit relaxation of the two-thirds yield peak stress limitation to a somewhat higher ratio. Furthermore, more detailed stress analysis might reveal a higher or lower nominal stress in the critical region of the coil case, depending on local detail effects. For example, it is believed that thick-beam stress effects, which definitely occur on the circular arcs, would raise the peak stresses above the present values which were computed using thin beam theory.

CONCLUSION AND RECOMMENDATIONS

The results of this study indicate the distinct advantage of intracoil connectors across the lobes of the major arc. However, for the present TMR, the reactor plasma fanshape occupies the space between the major arcs and so no structure can be placed there.

Most of the calculations performed in this study applied the conductor body forces directly to the case. However, some examples in which the conductor was allowed to deflect radially along the minor arc, without making contact with the case, were run. The small arc radial forces were then transferred to the case as inward radial loads on the major arc, which was a less highly stressed region. These analyses resulted in lower maximum case stresses. More detailed analyses, using a more refined structural model, could pinpoint an optimum configuration and further improve the design.

Our marginally acceptable final design is shown in Figures 3 and 5 with loads as in Figure 10,. and stresses as case 16.1 of Table 5 for the coil support structure. We used the continuous angle beam fastened to both coil cases, and stiffened with discrete gussets. In the vicinity of the small radius, the angle was built into a box section. This box section was 3 times as stiff as the angle alone and extended for approximately 40% of the coil pair. The proposed final design used design clearances in the minor arc to transfer loads via the conductor to the less highly stressed major arc.

It may be seen from this work that it should be possible to design an acceptable structural support system for a yin-yang end-plug in a tandem mirror reactor with thermal barriers. It is expected that more detailed design and analyses could be conducted to pinpoint an

optimum loading configuration and refine the overall case design.

References

1. R. W. Moir, et al, "Standard Mirror Fusion Reactor Design Study," Lawrence Livermore National Laboratory Report UCID-17644 (1978).

2. T. H. Batzer, et al, "Conceptual Design of a Mirror Reactor for a Fusion Engineering Research Facility (FERF)," Lawrence Livermore National Laboratory Report UCRL 51617 (1974).

3. G. A. Carlson, et al, "Tandem Mirror Reactor with Thermal Barriers," Lawrence Livermore National Laboratory Report UCRL-52836 (1979).

4. G. H. Henning, et al, "Mirror Fusion Test Facility Magnet," Lawrence Livermore National Laboratory Report UCRL 82890 (1979).

5. S. J. Sackett, "EFFI - A Code for Calculating the Electromagnetic Field, Force and Inductance in Coil Systems of Arbitrary Geometry," UCRL Report No. 52402 (March 1978).

6. "NASTRAN User's Manual, Level 17.0," NASA SP-222 (03) (March 1976).

Case No.	Description	Stress (ksi) At Center of Small Radius			
		P/A	Bending	Components	Peak
5	Stiff connections every 15° of arc between coils	67	84	4	155
9	Continuous angle connection between coils	40	109	20	168
12	Very stiff angle connection (10 x Case 9 stiffness) continuous	33	32	18	83
13	Similar to Case 12 but angle is stiff only over 60% of coil	33	59	13	105
14	Similar to Case 13 but only for 53% coil	33	65	13	111
15	Similar to Case 13 but only for 47%	34	70	14	119
16	40%-otherwise similar to 13	35	77	15	126
17	33%-otherwise similar to 13	35	83	16	134
18	27%-otherwise similar to 13	36	89	16	142
19	20%-otherwise similar to 13	37	95	17	149

MBO-1194-0169

Table 4 Intercoil and angle connection effects upon TMR yin yang peak stress for new coil case design

Case No.	Description	Max. Stress Components (ksi) at Center of Small Radius			
			Bending Components		
			Inplane	Out-of-Plane	Sum
4	Original loads (Fig. 9 Original angle properties	31	139	18	188
8	Original loads (Fig. 9 .3 x original angle properties	33	52	18	93
11	Original loads (Fig. 9 10 x angle properties for 40% of coil	35	77	15	126
9.1	New loads (Fig. 10) Angle connected softly to cases Original angle	13	113	21	147
9.2	Angle connected stiffly to cases	25	83	13	121
16.1	New loads (Fig. 10) 3 x original angle properties over 40% of coil	20	64	11	95
16.2	New loads (Fig. 10) 3 x original angle properties over 100% of coil	20	59	10	89

Table 5 Peak stresses in coil case with and without case/conductor clearances

DISCLAIMER

This document was prepared as an account of work sponsored by an agency of the United States Government. Neither the United States Government nor the University of California nor any of their employees, makes any warranty, express or implied, or assumes any legal liability or responsibility for the accuracy, completeness, or usefulness of any information, apparatus, product, or process disclosed, or represents that its use would not infringe privately owned rights. Reference herein to any specific commercial products, process, or service by trade name, trademark, manufacturer, or otherwise, does not necessarily constitute or imply its endorsement, recommendation, or favoring by the United States Government or the University of California. The views and opinions of authors expressed herein do not necessarily state or reflect those of the United States Government thereof, and shall not be used for advertising or product endorsement purposes.